J. Appl. Comput. Mech., 6(4) (2020) 908-919
DOI: 10.22055/JACM.2019.30065.1672

ISSN: 2383-4536
jacm.scu.ac.ir

M&MoCS

Shahid Chamran University of Ahvaz

Journal of Applied and Computational Mechanics

Research Paper

Free Vibration Analysis of Functionally Graded Beams with Cracks

Shkelzen Shabani[1,2], Yusuf Cunedioglu[2]

[1] Department of Production and Automation, Faculty of Mechanical Engineering, University of Prishtina "Hasan Prishtina"
10000 Prishtina, Kosovo, Email: shkelzen.shabani@uni-pr.edu

[2] Department of Mechanical Engineering, Faculty of Engineering, Nigde Omer Halisdemir University
51245 Nigde, Turkey, Email: ycunedioglu@ohu.edu.tr

Received June 24 2019; Revised August 29 2019; Accepted for publication October 24 2019.
Corresponding author: Shkelzen Shabani (shkelzen.shabani@uni-pr.edu)

Abstract. This study introduces the free vibration analysis of multilayered symmetric sandwich Timoshenko beams, made of functionally graded materials with two edge cracked, using the finite element method and linear elastic fracture mechanic theory. The FG beam consists of 50 layers, located symmetrically to the neutral plane, whose material properties distribution change along the beam thickness, according to power and exponential laws. The constituent of each layer of the beam is different, but each layer is isotropic and homogeneous. Natural frequency values of a cantilever beam are calculated using a developed MATLAB code. There is good agreement between the present results and the published results from the literature. A detailed study is carried out to observe the effect of crack location, crack depth ratio, power law index and material distribution on the first four natural frequencies.

Keywords: Functionally graded beam; Cracked beam; Free vibration; FEM.

1. Introduction

In 1984, a group of Japan scientists proposed the idea of functionally graded materials (FGMs), during the design of thermal barrier materials, for the aerospace needs [1]. In the FGMs, material properties change steady throughout the desired direction, providing a structural integrity. In general, FGMs consist of a mixture of a metal and a ceramic. In this manner, the metal ensures the strength and the toughness, while the ceramic endures high temperatures in a thermal environment and provides the corrosion resistance. The FGMs have been considerably used in different engineering branches such as: aerospace, civil, automotive, biomedical and other engineering structures.

There are many studies related to the vibration behavior of cracked beams [2]–[9]. Further, the authors studied dynamics and free vibrations characteristics of cracked and non-cracked FG beams and plates. For example, Aydogdu and Taskin [10] studied free vibration analysis of FG beams with the simply supported boundary conditions. Yang and Chen [11] introduced a theoretical study on free vibration and elastic buckling of FGM beams with open edge cracks with Bernoulli–Euler beam theory and the rotational spring model. Alshorbagy et al. [12] studied the dynamic characteristics of the FG beam using finite element method. Material distribution is assumed to vary axially or transversally through thickness according to the power law. The Euler-Bernoulli beam theory is used to derive the equation of motion. Şimşek et al. [13] analyzed the dynamic problem of an axially functionally graded beam using Euler Bernoulli beam theory as a result of a moving harmonic load. Yang et al. [14] studied free vibration of the FG sandwich beam using the two-dimensional elasticity theory based on mesh-free boundary-domain integral equation method. Su and Banerjee [15] studied the free vibration of FG Timoshenko beam by a developed dynamic stiffness developed

Published online: October 25 2019

method. Cunedioglu [16] studied the free vibration of symmetric sandwich FGM cracked beams using the finite element method, based on the Timoshenko beam theory. Material properties change in the thickness direction and are defined by an exponential and a polynomial functions. A massless and dimensionless spring element represents the cracked structure. The effects of crack location, crack depth, material distribution parameter (n) and beam thickness aspect ratio on natural frequencies were investigated in the study. Yilmaz and Evran [17] studied the free vibration behavior of short FG beams through experimental and finite element method. The Ansys software is used to model each layer of the beam, axially distributed, using Timoshenko beam theory. Chen and Chang [18] studied the free vibrations of the FG according to Euler-Bernoulli beam theory using a transformed section method by deriving closed-form solutions. Material properties change through the thickness direction according to a simple power law. Xing et al. [19] presented closed form solution for free vibration of rectangular FG plates in thermal environment for different boundary conditions. Song et al. [20] used a hybrid method to study vibration problems of a FG plate with a moving mass, based on improved Rayleigh-Ritz solution together with penalty method and differential quadrature method. Lien et al. [21] introduced free vibration study of multiple cracked FGM Timoshenko beam. Vibration equations were set by using the rotational spring model of cracks, dynamic stiffness method and the actual position of the neutral plane.

The presence of a crack causes a reduction in rigidity and this influences the dynamic behavior of the structure. The dynamic behavior of the structure must be known on beforehand if resonance of the structure has to be prevented. During the design stage one must take into consideration the natural frequencies of the structure. For that reason in this study, two edge cracked multilayered symmetric sandwich FG beams are investigated in terms of free vibration. The considered problem is carried out within the Timoshenko beam first order shear deformation theory by using the finite element method. It is assumed that the material properties distribution change along the beam thickness according to power and exponential laws. As a result, the novelty of this work is to estimate the natural frequencies of the two edge cracked FG beams by using the effective mass density and Young's modulus using mixture rules and laminate theory. Hence, natural frequencies are calculated by using the obtained effective material properties for two edge cracked cantilever boundary conditions. There is good accordance between the present results with the available ones from the literature. A detailed study is carried out to observe the effect of crack location, crack depth ratio and material distribution on the first four natural frequencies.

2. Functionally Graded Symmetric Sandwich Beam

An FG symmetric sandwich beam, with a rectangular cross-section, of length L, width d, thickness b and the number of the layers N, is considered and shown in Fig. 1. To have more realistic solutions, the considered beam consists of fifty layers. Each layer is composed of a mixture of aluminum (Al) and alumina phases (Al_2O_3), arranged symmetrically to the neutral axis of the beam. The upper and the lower part of the beam layers are made of pure ceramic (Al_2O_3), the middle part is pure metal (Al), while the layers between them are made of FGM.

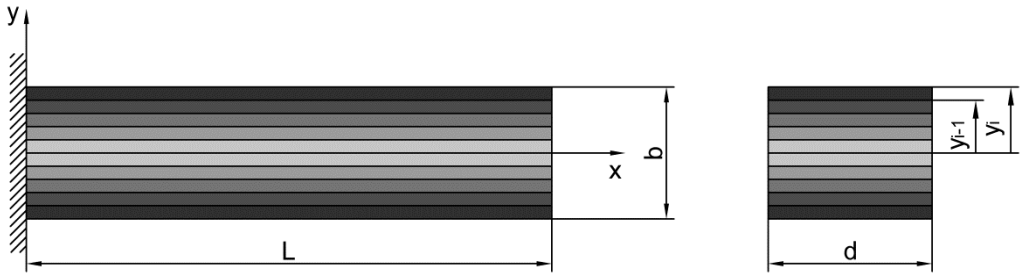

Fig. 1. Symmetric FG sandwich beam.

Polynomial or exponential functions are used to set the mixture ratio, which varies continuously from the upper and the lower part toward the beam neutral plane.

The material properties of the beam such as Young's modulus and the density, are first calculated for the upper half using the exponential and power laws equations [1] and then throughout the whole thickness of the beam using the laminate theory.

$$E(y) = E_c e^{(-\delta(1-2y))}, \delta = \frac{1}{2}\ln\left(\frac{E_c}{E_m}\right) \tag{1}$$

$$E(y) = (E_c - E_m)\left(y + \frac{1}{2}\right)^n + E_m \tag{2}$$

where E_c, E_m, y and n are Young's modulus of ceramic, metal, the coordinate axis and power law index, respectively. The same equations are also used for density:

$$\rho(y)=\rho_c e^{(-\delta(1-2y))}, \delta=\frac{1}{2}\ln\left(\frac{\rho_c}{\rho_m}\right) \tag{3}$$

$$\rho(y)=(\rho_c-\rho_m)\left(y+\frac{1}{2}\right)^n+\rho_m \tag{4}$$

where ρ_c and ρ_m are the mass density for ceramic and metal, respectively.

The variable y is defined as: $y=-\frac{1}{2},-\frac{1}{2}+\frac{1}{\eta},-\frac{1}{2}+\frac{2}{\eta},\ldots,\frac{1}{2}$, where $\eta=\frac{N}{2}-1$ and N is the number of layers. The effective Young's modulus and mass density of the whole beam are calculated using laminate theory, by following formulas [22]:

$$E_{ef}=\frac{8}{b^3}\sum_{i=1}^{N/2}\left(E_y\right)_i\left(y_i^3-y_{i-1}^3\right) \tag{5}$$

$$\rho_{ef}=\frac{8}{b^3}\sum_{i=1}^{N/2}\left(\rho_y\right)_i\left(y_i^3-y_{i-1}^3\right) \tag{6}$$

3. Stiffness and Mass Matrices of the Timoshenko Beam Element

The procedures for developing stiffness and mass matrices of a two node beam, with 2 degrees of freedom $\delta=\{v,\theta\}$ at each node, are provided by Logan [23]. In Fig. 2, it is shown a general beam finite element, with all applied forces (F_1, F_2, F_3, F_4, F_5, F_6) and corresponding displacements (u_1, v_1, θ_1, u_2, v_2, θ_2).

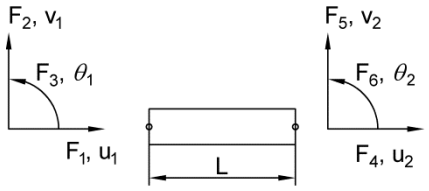

Fig. 2. Division of the beam components into finite elements.

$$[K_1]=\frac{EI}{L\left(L^2+12g\right)}\begin{bmatrix}12 & 6L & -12 & 6L\\ 6L & \left(4L^2+12g\right) & -6L & \left(2L^2-12g\right)\\ -12 & -6L & 12 & -6L\\ 6L & \left(2L^2-12g\right) & -6L & \left(4L^2+12g\right)\end{bmatrix} \tag{7}$$

$$[M_1]=\frac{\rho AL}{420(1+\zeta)^2}\begin{bmatrix}m_1 & Lm_2^2 & m_3 & -Lm_4\\ Lm_2^2 & Lm_5^2 & Lm_4 & -Lm_6^2\\ m_3 & Lm_4 & m_1 & -Lm_2^2\\ -Lm_4 & -lm_6^2 & -Lm_2^2 & Lm_5^2\end{bmatrix}+\frac{\rho I}{30L(1+\zeta)^2}\begin{bmatrix}m_7 & Lm_8 & -m_7 & Lm_8\\ Lm_8 & L^2m_9 & -Lm_8 & -L^2m_{10}\\ -m_7 & -Lm_8 & m_7 & -Lm_8\\ Lm_8 & -L^2m_{10} & -Lm_8 & L^2m_8\end{bmatrix} \tag{8}$$

where L is the length of the beam, E is Young's modulus and I_z is the section moment of inertia to z-axis, $\zeta=x/L,\tau=12g/L^2$.

$$g=\frac{EI}{k_sAG} \tag{9}$$

where k_s is shear correction factor, A is beam cross-section, G is shear modulus and we have:

$$m_1=\frac{1}{420(1+\tau)^2}\left(156+294\tau+140\tau^2\right),\ m_2=\frac{1}{420(1+\tau)^2}\left(22+38.5\tau+17.5\tau^2\right),$$
$$m_3=\frac{1}{420(1+\tau)^2}\left(54+126\tau+70\tau^2\right),\ m_4=\frac{-L}{420(1+\tau)^2}\left(13+31.5\tau+17.5\tau^2\right), \tag{10}$$

$$m_5=\frac{L^2}{420(1+\tau)^2}\left(4+7\tau+3.5\tau^2\right),\ m_6=\frac{-L^2}{420(1+\tau)^2}\left(3+7\tau+3.5\tau^2\right),\ m_7=\frac{36}{30L^2(\tau+1)^2},$$

$$m_8=\frac{3-15\tau}{30L(\tau+1)^2},\ m_9=\frac{4+5\tau+10\tau^2}{30(\tau+1)^2},\ m_{10}=-\frac{1+5\tau-5\tau^2}{30(\tau+1)^2}$$

The stiffness and mass matrices for a beam having 1 degree of freedom, local axial displacement, in the x-direction, developed by Logan [23], are as follows:

$$[K_2]=\frac{EA}{L}\begin{bmatrix}1 & -1\\ -1 & 1\end{bmatrix} \tag{11}$$

$$[M_2]=\frac{\rho\cdot A\cdot L}{6}\begin{bmatrix}2 & 1\\ 1 & 2\end{bmatrix} \tag{12}$$

Using the above-obtained K_1, K_2, M_1 and M_2 matrices, the total stiffness and mass matrices for 3 degrees of freedom at each node become:

$$K_{el}=\begin{bmatrix}K_2 11 & & & K_2 12 & & \\ & K_1 11 & K_1 12 & & K_1 13 & K_1 14\\ & K_1 21 & K_1 22 & & K_1 23 & K_1 24\\ K_2 21 & & & K_2 22 & & \\ & K_1 31 & K_1 32 & & K_1 33 & K_1 34\\ & K_1 41 & K_1 42 & & K_1 43 & K_1 44\end{bmatrix}_{(6\times 6)} \tag{13}$$

$$M_{el}=\begin{bmatrix}M_2 11 & & & M_2 12 & & \\ & M_1 11 & M_1 12 & & M_1 13 & M_1 14\\ & M_1 21 & M_1 22 & & M_1 23 & M_1 24\\ M_2 21 & & & M_2 22 & & \\ & M_1 31 & M_1 32 & & M_1 33 & M_1 34\\ & M_1 41 & M_1 42 & & M_1 43 & M_1 44\end{bmatrix}_{(6\times 6)} \tag{14}$$

4. The Stiffness Matrix for the Crack

In this study, the cracked node as a cracked element of zero mass and zero length is considered to represent the crack [7]. Using the flexibility coefficient according to the displacement vector $\delta=\{u,v,\theta\}$, we write compliance coefficient matrix [6].

$$C=\begin{bmatrix}c_{11} & 0 & c_{13}\\ 0 & c_{22} & 0\\ c_{31} & 0 & c_{33}\end{bmatrix}_{(3\times 3)} \tag{15}$$

The inverse of the above compliance matrix is the stiffness matrix of the nodal point. In the end, the crack stiffness matrix is as follows:

$$K_{cr}=\begin{bmatrix}[C]^{-1} & -[C]^{-1}\\ -[C]^{-1} & [C]^{-1}\end{bmatrix}_{(6\times 6)} \tag{16}$$

The eigenvalue expressions of free vibration of an intact [24] and cracked beam [25] are as follows;

$$\left([K]-\omega^2[M]\right)\{\bar{d}\}=0 \tag{17}$$

$$\left(([K]+[K_{cr}])-\omega^2[M]\right)\{\bar{d}\}=0 \tag{18}$$

where $[K]$ is the global stiffness matrix, $[M]$ is the global mass matrix, ω is the natural angular frequency in radians

per second, and $\{\bar{d}\}$ the mode shape.

5. Verification of the Two Cracked Cantilever Beam Model

To verify the correctness of the suggested approach and the finite element MATLAB code, an example from the literature [26] is considered. The geometric dimensions of the considered two cracked beam are indicated in Fig. 3, with length L=0.8 m, width d=0.02 m, height b=0.02 m, first crack location Lc_1 = 0.12 m, first crack depth a_1=0.002 m, second crack location Lc_2=0.4 m and second crack depth a_2=0.003 m. Material properties are as follows: Young's modulus E=210 GPa and density ρ=7800 kg/m^3. In the study, Timoshenko beam theory is used. Since it is not mentioned in the literature, the following parameters are assumed: shear stiffness modulus G=3/8E, Poisson's ratio ν =0.28 and the shape correction factor κ=5/6.
As can be seen from Table 1, the obtained results in this study are consistent with those in the literature.

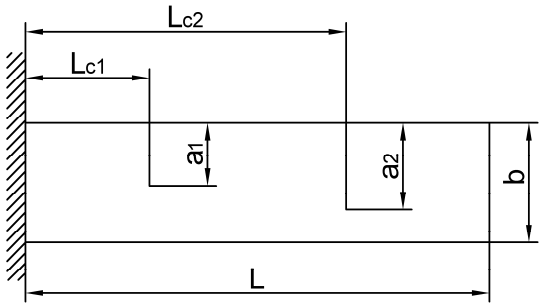

Fig. 3. Two cracked cantilever beam model.

Table 1. The first three natural frequencies of the two cracked cantilever beam.

Natural frequency	Lc_1 (m)	a_1 (m)	Lc_2 (m)	a_2 (m)	Shifrin and Ruotolo [26] (Hz)	This study (Hz)
1	0.12	0.002	0.4	0.003	26.0591	26.04356
2	0.12	0.002	0.4	0.003	162.5727	162.4123
3	0.12	0.002	0.4	0.003	455.9487	455.8614

6. Verification of the Un-cracked/Cracked Functionally Graded Beam

The material properties are assumed to vary along the thickness of the beam, characterized by 50 layers, symmetrical to the neutral axis. The calculation of the natural frequencies is done according to the Timoshenko beam theory, considering the effects of the rotary inertia and shear deformation. For the verification of the results, a literature example [16] is considered (Fig. 4). The assumed beam is of length L=200 mm, thickness b=5 mm and width d=20 mm.

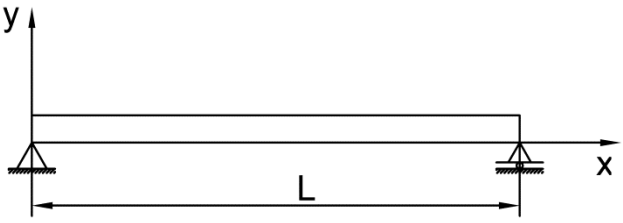

Fig. 4. Simply supported symmetric FG sandwich beam.

Table 2. Material properties of the constituents of the beam.

Material	E (GPa)	ρ (kg/m3)	ν
Al	70	2700	0.3
Al_2O_3	380	3950	0.3

Material properties of the Aluminium (Al) and the Ceramic (Al_2O_3), are given in Table 2 [16]. In order to satisfy convergence, the number of elements used to generate finite element models is 100. Exponential and polynomial functions are used to perform the analysis. The first four natural frequency values are given in Table 3.
As can be seen from Table 3, the natural frequency values calculated with MATLAB code show good agreement with the literature.

Table 3. The first four natural frequencies (Hz) of a simply supported FG sandwich Timoshenko beam.

Function			Mode 1	Mode 2	Mode 3	Mode 4
Exponential		Demir et al. [1]	486.52	1939.6	4341.8	7663.15
		Present	486.422	1939.445	4340.726	7660.899
Polynomial	n=0.1	Demir et al. [1]	550.91	2196.89	4917.36	8679.65
		Present	550.944	2196.707	4916.511	8677.095
	n=0.5	Demir et al. [1]	534.98	2133.31	4775.06	8428.46
		Present	534.999	2133.135	4774.228	8425.982
	n=1	Demir et al. [1]	518.2	2065.88	4624.09	8162
		Present	518.086	2065.695	4623.289	8159.592
	n=5	Demir et al. [1]	443.06	1766.61	3954.27	6979.69
		Present	443.038	1766.469	3953.582	6977.634
	n=10	Demir et al. [1]	404.67	1613.63	3611.82	6375.24
		Present	404.671	1613.492	3611.200	6373.368

Furthermore, a commercial program ANSYS is used to support presented results for a two cracked functionally graded beam using the finite element method. The fifty layer beam is modeled in INVENTOR program and exported to ANSYS. Material properties, such as Young's modulus and the density have been assigned to each layer of the upper half of the beam using exponential and power laws functions from the equation 1 to 4, while the poisons ratio is taken as a constant value of 0.3. Since the beam is symmetric the same values have been assigned also for the lower part of the beam. The beam is meshed by SOLID186 element which is defined by 20 nodes having three degrees of freedom per node. The crack is defined as a zero thickness surface, and the boundary conditions are chosen for the cantilever type beam. The block Lanczos method is used for the eigenvalue extractions to calculate frequencies. The material properties and the geometric dimensions of the beam are the same as the un-cracked simply supported FG beam, while the values of the supposed cracks are as follows: the first crack location (Lc_1/L=0.2), second crack location (Lc_2/L=0.4), first crack ratio (a_1/b=0.4) and the second crack ratio (a_2/b=0.4). The MATLAB model is the same as the ANSYS one.
As can be seen from Table 4, the natural frequency values calculated with MATLAB code show good agreement with the ANSYS. The difference between the results is due to the method selection and fine refinement of the mesh in the ANSYS.

Table 4. The first four natural frequencies (Hz) of a two cracked cantilever FG sandwich Timoshenko beam.

Function			Mode 1	Mode 2	Mode 3	Mode 4
Exponential		Matlab	162.564	1052.729	2924.263	5630.451
		Ansys	162.050	1070.200	2994.900	5592.500
Polynomial	n=0.1	Matlab	184.128	1192.371	3312.158	6377.314
		Ansys	184.200	1200.700	3348.000	6387.800
	n=0.5	Matlab	178.799	1157.864	3216.305	6192.756
		Ansys	179.800	1179.800	3291.400	6224.600
	n=1	Matlab	173.147	1121.258	3114.620	5996.969
		Ansys	173.580	1143.600	3198.900	5993.700
	n=5	Matlab	148.065	958.838	2663.452	5128.278
		Ansys	147.200	970.740	2715.700	5065.700
	n=10	Matlab	135.243	875.802	2432.796	4684.167
		Ansys	134.950	884.590	2472.300	4649.300

7. Numerical Results

In this section, several detailed cases are provided to show the effects of the crack location, crack depth ratio, power law index (n) and the different material distribution on the first four natural frequencies. For the purposes of the analysis, a two edge cracked isotropic homogeneous cantilever beam (Fig. 3), is assumed to be a symmetric sandwich FG Timoshenko beam. The geometric parameters, the material properties and the number of elements that provide the convergence of the assumed beam are considered to be the same as those used in verification of the FG beam (see: section 6). The beam consists of 50 layers, rectangular cross-section, where the material properties of the FG beam are assumed to change in the thickness direction according to the exponential and the power laws.

Case 1. $Lc1/L$, a_1/b – constant.

In this case, the effects of the second crack location (Lc_2/L) and the second crack depth ratio (a_2/b) on the first four natural frequencies, in a cracked cantilever FG beam, are analyzed. Material properties of the FG beam change in the thickness direction, according to the exponential and the polynomial function. The first crack location (Lc_1/L=0.2) and the first crack ratio (a_1/b=0.2) are considered constant. The graphs for the polynomial function are given only for the power law index (n=5).
From Fig. 5a and b, one can observe an increase in the 1st natural frequency values as the second crack location (Lc_2/L) approaches the free end of the beam. On the other side, the increase of the second crack ratio (a_2/b) causes a decrease in the 1st natural frequency values.

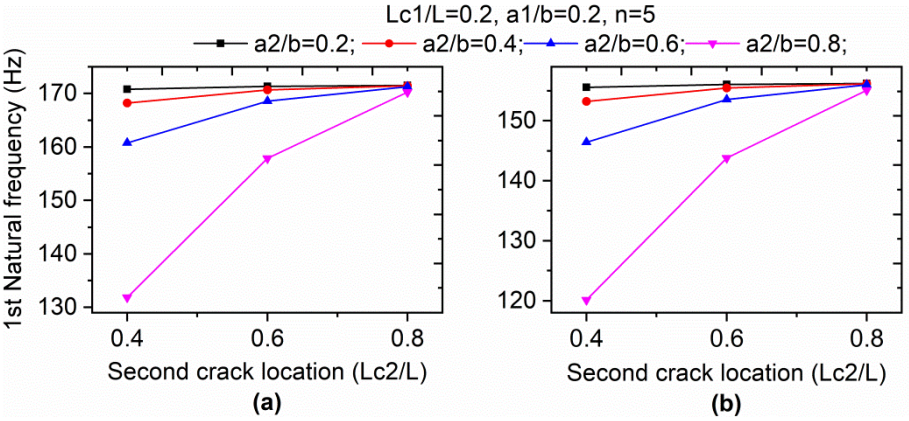

Fig. 5. The effects of the second crack location (Lc_2/L) and the second crack depth ratio (a_2/b) on the 1st natural frequency values of (a) exponential and (b) polynomial functions.

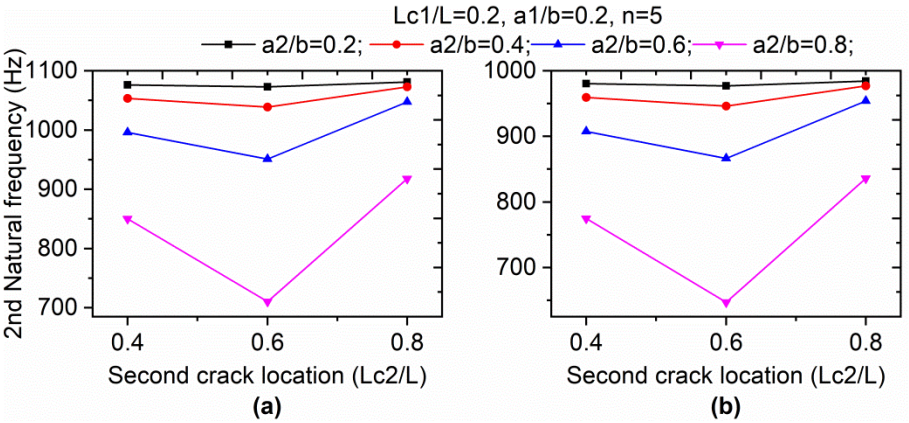

Fig. 6. The effects of the second crack location (Lc_2/L) and the second crack depth ratio (a_2/b) on the 2nd natural frequency values of (a) exponential and (b) polynomial functions.

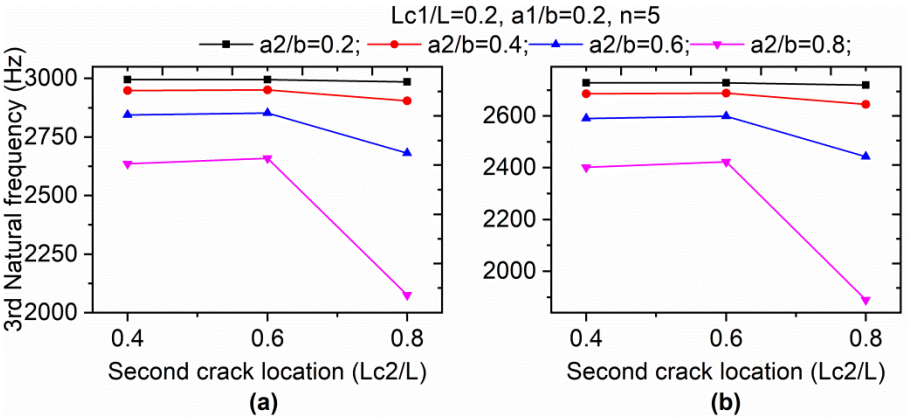

Fig. 7. The effects of the second crack location (Lc_2/L) and the second crack depth ratio (a_2/b) on the 3rd natural frequency values of (a) exponential and (b) polynomial functions.

For the second crack location (Lc_2/L=0.6), the 2nd natural frequency attains minimum values (Fig. 6a, b), while the 3rd natural frequency attains maximum values (Fig. 7a, b). However, as it can be seen in both figures, the natural frequencies decrease as the second crack ratio (a_2/b) increases.

From Fig. 8a and b, one can observe that increasing of the second crack depth ratio (a_2/b) and shifting of the second crack location (Lc_2/L) toward the free end of the beam, the values of the 4th natural frequency decrease.

Case 2. Lc_1/L, Lc_2/L – constant.

Analyzes were conducted to see the effects on natural frequency values, when changing the first (a_1/b) and the second (a_2/b) crack depth ratio. The first crack location (Lc_1/L=0.2) and the second crack location (Lc_2/L=0.4) are considered constant. From Fig. 9 and Fig. 10, one can observe that all natural frequencies decrease as both crack ratios increase. However, as shown in Fig. 9b and Fig. 10b, the 2nd natural frequencies are less affected by the change of the first and second crack depth ratio.

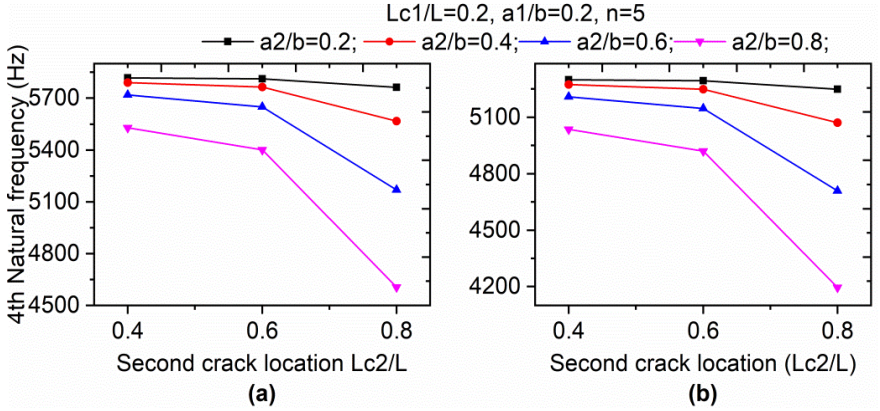

Fig. 8. The effects of the second crack location (Lc_2/L) and the second crack depth ratio (a_2/b) on the 4th natural frequencies values of (a) exponential and (b) polynomial functions.

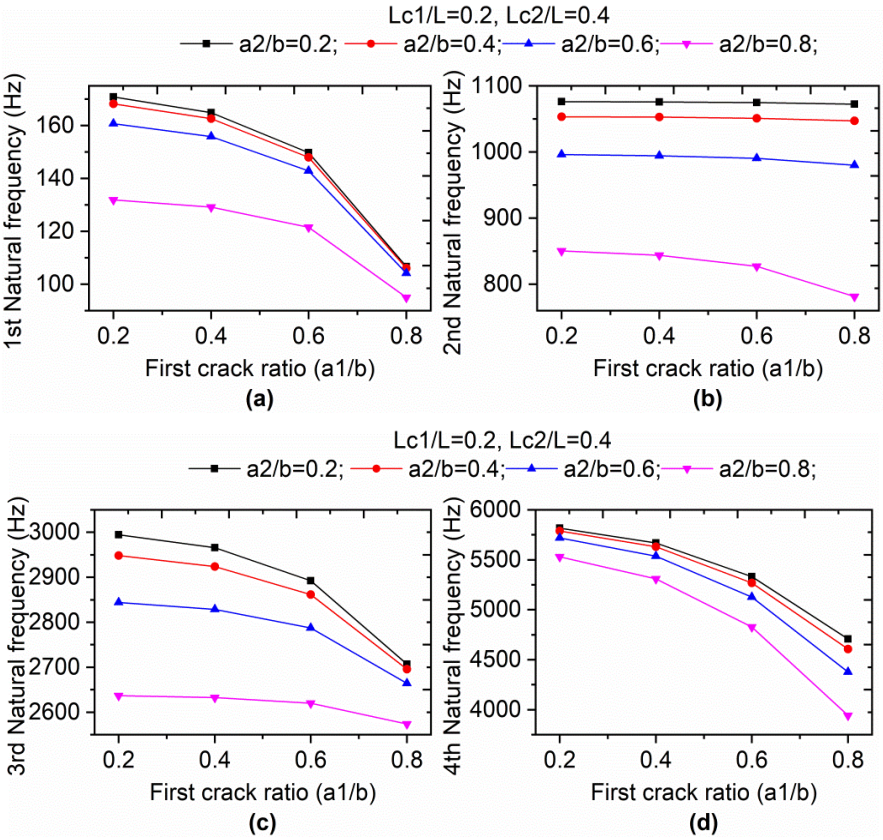

Fig. 9. The effects of the first crack ratio (a_1/b) and second crack depth ratio (a_2/b) on the first four natural frequency values for the exponential function.

Case 3. Lc_1/L, a_1/b, Lc_2/L– constant.

The effects of the power index (n) and the second crack depth ratio (a_2/b) on the natural frequencies, are analyzed by considering Lc_1/L=0.2, a_1/b=0.2 and Lc_2/L=0.4 constant. From Fig. 10 one can observe that all natural frequencies decrease as the power index (n) and the second crack depth ratio increase.

Case 4. Lc_1/L, Lc_2/L, a_2/b – constant.

To analyze the effects of the first crack ratio (a_1/b) and the power index (n) on natural frequencies, the values of Lc_1/L=0.2, Lc_2/L=0.4 and a_2/b=0.2 are considered constant. As shown in Fig. 11, all natural frequency values decrease as the first crack ratio and the power index increase. However, the 2nd natural frequencies are less affected from the variation of the first crack ratio.

Case 5. Lc_1/L, a_1/b, a_2/b – constant.

In this case are shown the effects of the second crack location (Lc_2/L) and the power index (n) on natural frequencies, when Lc_1/L=0.2, a_1/b=0.2 and a_2/b=0.2 are considered constant. As shown in the Fig. 12a and d, when the second crack location approaches the free end of the beam, there is a slight increase in the 1st natural frequencies, and slight decrease in the 4th natural frequencies, respectively. As shown in the Fig. 12b and c, for the second crack location (Lc_2/L=0.6), the

2nd natural frequencies attain the minimum values, while the 3rd natural frequencies attain the maximum values, respectively. From the Fig. 12, all natural frequencies decrease as the power index increases.

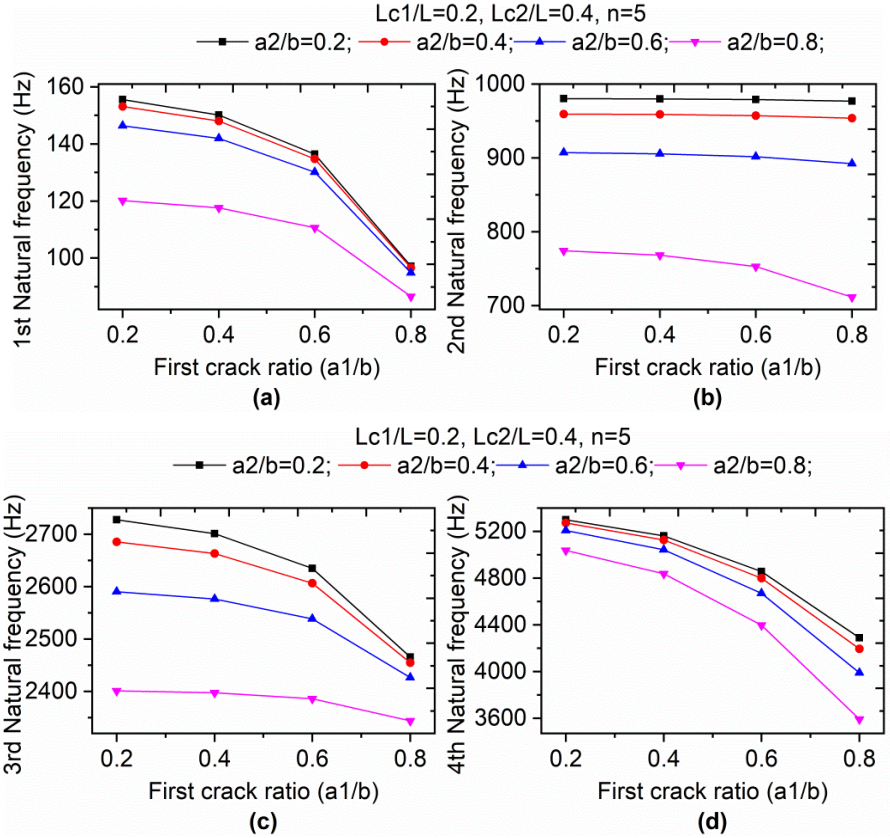

Fig. 10. The effects of the first crack ratio (a_1/b) and second crack depth ratio (a_2/b) on the first four natural frequency values for the polynomial function.

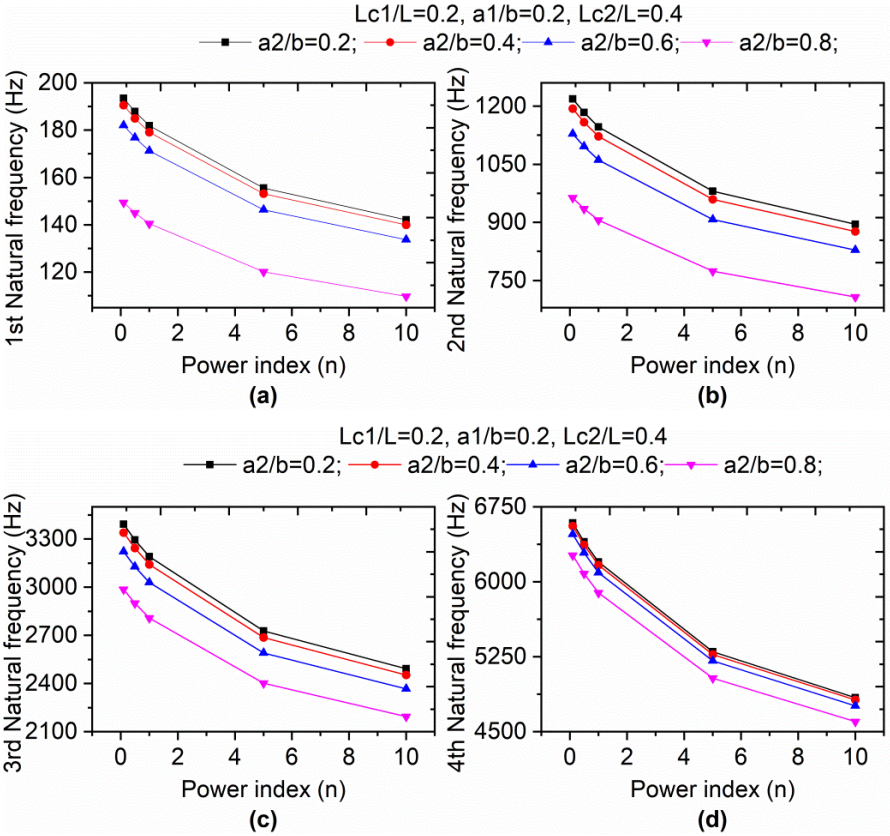

Fig. 11. The effects of the power index (n) and second crack depth ratio (a_2/b) on the first four natural frequencies values.

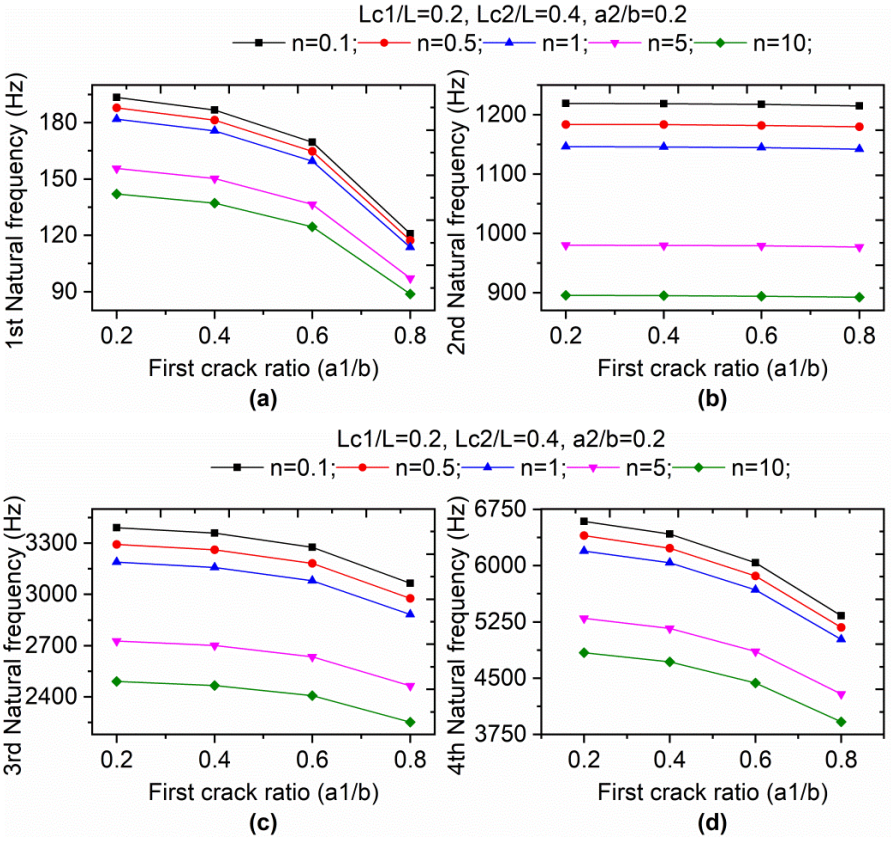

Fig. 12. The effect of the first crack ratio (a_1/b) and the power index (n) on the first four natural frequency values.

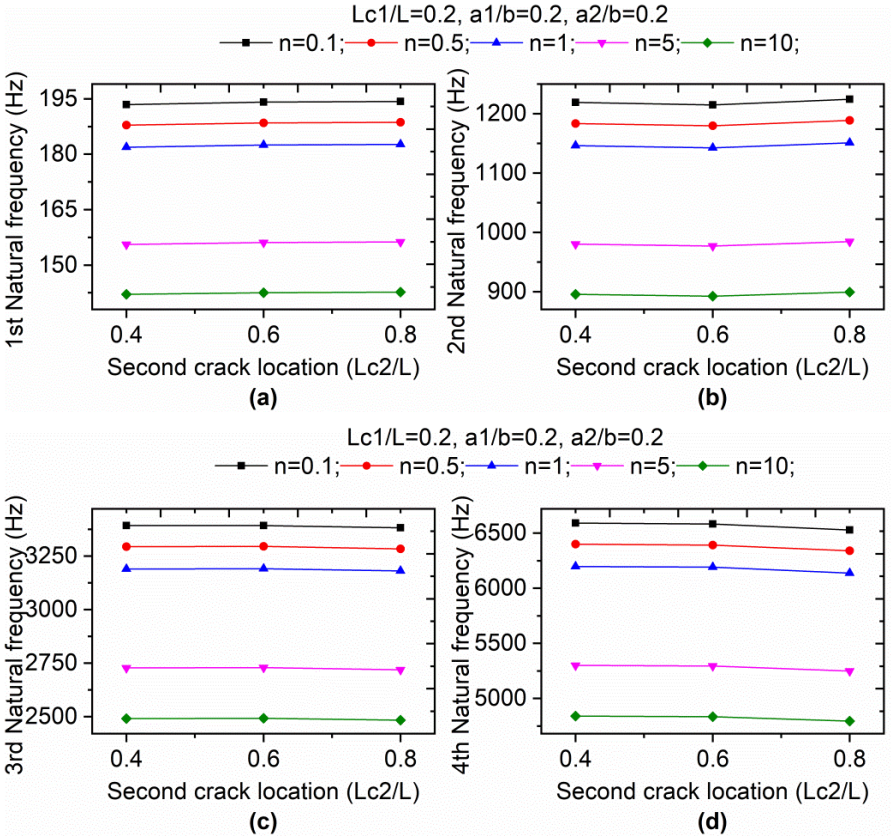

Fig. 13. The effect of the power index (n) and second crack location (Lc_2/L) on the first four natural frequency values.

When the theoretical background is examined, it can be seen that the stiffness and mass matrix are a function of the polynomial degree n. On the other hand the crack stiffness matrix is a function of the crack ratio and crack location. The variation of the natural frequencies in Fig. 5-13 can be explained by the aforementioned reasons.

8. Conclusion

Free vibrations of the two edge cracked cantilever symmetric FG sandwich Timoshenko beam was investigated. The study observed in detail the effects of the crack location, crack depth ratio, power index (n) and different material distributions on the first four natural frequencies. Some of the obtained results are presented as follows:

- The change in the crack location causes changes in the natural frequency values.
- Increasing the crack ratio causes a decrease in the natural frequency values.
- Increasing the power index (n) causes a decrease in the natural frequency values, whereas the change of the second crack location (Lc_2/L) has limited effects on the natural frequency values.
- The change of the power index (n) affects the natural frequency values, while the first crack ratio (a_1/b) has little effect on the 2nd natural frequency values.

Author Contributions

S. Shabani developed the mathematical modeling and examined the theory; Y. Cunedioglu developed the MATLAB code and validated the code with literature. The manuscript was written through the contribution of all authors. All authors discussed the results, reviewed and approved the final version of the manuscript.

Conflict of Interest

The authors declared no potential conflicts of interest with respect to the research, authorship and publication of this article.

Funding

The authors received no financial support for the research, authorship and publication of this article.

References

[1] E. Demir, H. Çallioğlu, and M. Sayer, Free vibration of symmetric FG sandwich Timoshenko beam with simply supported edges, *Indian J. Eng. Mater. Sci.*, 20(6), 2013, 515–521.

[2] J. Liu, Y. M. Shao, and W. D. Zhu, Free vibration analysis of a cantilever beam with a slant edge crack, *Proc. Inst. Mech. Eng. Part C J. Mech. Eng. Sci.*, 231(5), 2017, 823–843.

[3] M. Attar, A. Karrech, and K. Regenauer-Lieb, Dynamic response of cracked Timoshenko beams on elastic foundations under moving harmonic loads, *J. Vib. Control*, 23(3), 2017, 432–457.

[4] J. A. Loya, L. Rubio, and J. Fernández-Sáez, Natural frequencies for bending vibrations of Timoshenko cracked beams, *J. Sound Vib.*, 290(3–5), 2006, 640–653.

[5] D. Y. Zheng and N. J. Kessissoglou, Free vibration analysis of a cracked beam by finite element method, *J. Sound Vib.*, 273(3), 2004, 457–475.

[6] M. Kisa and J. Brandon, Free vibration analysis of multiple open-edge cracked beams by component mode synthesis, *J. Sound Vib.*, 238(1), 2000, 1–18.

[7] M. Kisa, J. Brandon, and M. Topcu, Free vibration analysis of cracked beams by a combination of finite elements and component mode synthesis methods, *Comput. Struct.*, 67(4), 1998, 215–223.

[8] M. H. H. Shen and C. Pierre, Free Vibrations of Beams With a Single-Edge Crack, *J. Sound Vib.*, 170(2), 1994, 237–259, 1994.

[9] J. Zeng, H. Ma, W. Zhang, and B. Wen, Dynamic characteristic analysis of cracked cantilever beams under different crack types, *Eng. Fail. Anal.*, 74, 2017, 80–94.

[10] M. Aydogdu and V. Taskin, Free vibration analysis of functionally graded beams with simply supported edges, *Mater. Des.*, 28(5), 2007, 1651–1656.

[11] J. Yang and Y. Chen, Free vibration and buckling analyses of functionally graded beams with edge cracks, *Compos. Struct.*, 83(1), 2008, 48–60.

[12] A. E. Alshorbagy, M. A. Eltaher, and F. F. Mahmoud, Free vibration characteristics of a functionally graded beam by finite element method, *Appl. Math. Model.*, 35(1), 2011, 412–425.

[13] M. Şimşek, T. Kocatürk, and Ş. D. Akbaş, Dynamic behavior of an axially functionally graded beam under action of a moving harmonic load, *Compos. Struct.*, 94(8), 2012, 2358–2364.

[14] Y. Yang, C. C. Lam, K. P. Kou, and V. P. Iu, Free vibration analysis of the functionally graded sandwich beams by a meshfree boundary-domain integral equation method, *Compos. Struct.*, 117(1), 2014, 32–39.

[15] H. Su and J. R. Banerjee, Development of dynamic stiffness method for free vibration of functionally graded Timoshenko beams, *Comput. Struct.*, 147, 2015, 107–116.

[16] Y. Cunedioglu, Free vibration analysis of edge cracked symmetric functionally graded sandwich beams, *Struct. Eng. Mech.*, 56(6), 2015, 1003–1020.

[17] Y. Yilmaz and S. Evran, Free vibration analysis of axially layered functionally graded short beams using experimental and finite element methods, *Sci. Eng. Compos. Mater.*, 23(4), 2016, 453–460.

[18] W. R. Chen and H. Chang, Closed-Form Solutions for Free Vibration Frequencies of Functionally Graded Euler-Bernoulli Beams, *Mech. Compos. Mater.*, 53(1), 2017, 79–98.
[19] Y. F. Xing, Z. K. Wang, and T. F. Xu, Closed-form Analytical Solutions for Free Vibration of Rectangular Functionally Graded Thin Plates in Thermal Environment, *Int. J. Appl. Mech.*, 10(3), 2018, 1850025.
[20] D. Song, J. Shi, and Z. Liu, Vibration analysis of functionally graded plate with a moving mass, *Appl. Math. Model.*, 46, 2017, 141–160.
[21] T. Van Lien, N. T. Duc, and N. T. Khiem, Free vibration analysis of multiple cracked functionally graded Timoshenko beams, *Lat. Am. J. Solids Struct.*, 14(9), 2017, 1752–1766.
[22] E. Demir, H. Çallioğlu, and M. Sayer, Free vibration of symmetric FG sandwich Timoshenko beam with simply supported edges, *Indian J. Eng. Mater. Sci.*, 20(6), 2013, 515–521.
[23] R. F. Gibson, *Principles of Composite Materials*. New York: McGraw-Hill, 1994.
[24] D. L. Logan, *A first course in the finite element method*, 4th ed. Toronto: Thomson, 2007.
[25] Y. Cunedioglu and B. Beylergil, Free vibration analysis of laminated composite beam under room and high temperatures, *Struct. Eng. Mech.*, 51(1), 2014, 111–130.
[26] Ş. D. Akbaş, Free vibration characteristics of edge cracked functionally graded beams by using finite element method, *Int. J. Eng. Trends Technol.*, 4(10), 2013, 4590–4597.
[27] E. I. Shifrin and R. Ruotolo, Natural frequencies of a beam with an arbitrary number of cracks, *J. Sound Vib.*, 222(3), 1999, 409–423.

ORCID iD

Shkelzen Shabani https://orcid.org/0000-0003-3852-9711
Yusuf Cunedioglu https://orcid.org/0000-0002-3424-0454